

GMI in the reentrant spin-glass $\text{Fe}_{90}\text{Zr}_{10}$ alloy: investigation of the spin dynamics in the MHz frequency regimeP.R.T. Ribeiro,¹ J. M. M. Ramírez,¹ R. Vidyasagar,¹ F. L. A. Machado,^{1, a)} S. M. Rezende,¹ and E. Dan Dahlberg²¹⁾ Departamento de Física, Universidade Federal de Pernambuco, 50670-901, Recife, Pernambuco, Brazil.²⁾ School of Physics and Astronomy, University of Minnesota, 55455, Minneapolis, Minnesota, USA.

(Dated: 29 August 2016)

Giant magnetoimpedance (GMI) in the reentrant spin-glass (SG) phase of ferromagnetic $\text{Fe}_{90}\text{Zr}_{10}$ is reported. The temperature (T) dependence of the GMI allows the investigation of the spin dynamics in the SG phase in the MHz frequency regime and thus very short relaxation times τ ($\sim 10^{-8}$ s). The GMI shows a broad maximum around 150 K and diminishes with decreasing T below the glass temperature T_g of 15 K. The magnetic permeability data obtained from the GMI data shows the general features observed in the ac magnetic susceptibility measured at lower frequencies ($10 \leq f \leq 10^4$ Hz), yielding values of T_f ($= T_g(f)$) that allow testing the validity of the power-law scaling used for describing the dynamics of SG-phases up to 15 MHz. A log-log plot of τ ($= 1/f$) versus the reduced critical temperature shows two distinct regimes in the time-domain: (1) a critical slowing-down is observed for values $\tau > 3 \times 10^{-3}$ s; and (2) for $7 \times 10^{-8} \leq \tau \leq 3 \times 10^{-3}$ s. In the later case a fitting to the power-law yields the value 7.4 for the product of the critical exponents $z\nu$, and 1.6×10^{-7} s for the microscopic relaxation time τ_0 . The product of the exponents is appropriate for an Ising spin glass.

PACS numbers: 75.50.Cc, 75.50.Lk, 75.50.Kj, 75.47.-m

Keywords: Spin-glass, ferromagnetism, giant magnetoimpedance, amorphous alloy

The physics resulting from competing interactions in magnetic materials responsible for the spin-glass state continue to be at the forefront of condensed matter physics. The interest comes from the subtle phase transitions, coexistence of the spin-glass state and ferromagnetic order, and associated dynamics; although extensively studied, these continue to defy experimentalists and theoreticians.^{1,2} As an example of early experiments in this area, Mössbauer data obtained for the metallic amorphous alloy $\text{Au}_{19}\text{Fe}_{81}$ showed ferromagnetic order below a Curie temperature T_C of 170 K followed by a spin-glass-like freezing below about 60 K.³ In this material a strong irreversibility in the magnetizations measured after cooling with an applied magnetic field (FC) and with zero field (ZFC) occurs below 15 K. As typifies a spin-glass, a cusp was also reported⁴ in the ac magnetic susceptibility in other work on this system. Similar behaviors have been observed in insulating disordered alloys such as $\text{Fe}_x\text{Zn}_{1-x}\text{F}_2$.⁵

Another important signature of the spin-glass phase that gives a clue to the nature of the magnetic interactions is the critical slowing-down of the spin dynamics.⁶ However, probing the spin-glass dynamics by direct measurement of the ac magnetic susceptibility has been largely limited by the experimental limitations to a few tens of kHz only.

In this paper we report a study of the spin dynamics in the MHz regime of the reentrant spin-glass state in

a $\text{Fe}_{90}\text{Zr}_{10}$ alloy employing the giant magnetoimpedance effect (GMI).⁷ The GMI is a measure of the frequency, magnetic field, and temperature dependent magnetic permeability, μ_T , through the penetration-depth $\delta = [\rho/(\pi f \mu_T)]^{1/2}$, where f is the frequency of an ac electric current applied to the sample and ρ is the electric resistivity.^{8,9} By measuring the GMI one can determine δ and find the dependence of the real and imaginary parts of the magnetic susceptibility $\chi_{ac} = \mu_T - 1 = \chi'_{ac} + i\chi''_{ac}$ as a function of the frequency, f , temperature, T , and applied magnetic field H . These measurements of the frequency dependent GMI provide direct information on the spin dynamics of the system being studied. In addition, for some technological applications the investigation of the temperature dependence of the GMI is of great importance.¹⁰⁻¹²

The phase diagram of the FeZr alloys is somewhat complex and, as expected, the transitions temperatures T_C and T_g are sensitive to the atomic percent of Zr.¹³⁻¹⁶ For $\text{Fe}_{90}\text{Zr}_{10}$ the low- T in-phase component of the ac magnetic susceptibility χ'_{ac} was found to decrease monotonically with T while a cusp with a maximum near 15 K that shifts to higher temperatures with increasing f was observed in the out-of-phase component χ''_{ac} .¹⁷ These ac susceptibility measurements of $\text{Fe}_{90}\text{Zr}_{10}$ were made with a Physical Properties Measurements System (PPMS-Quantum Design) for temperatures in the range 1.8 - 30 K. Examples of the data obtained with an ac magnetic field $h_{ac} = 5$ Oe and with f varying from 10 Hz to 10^4 Hz are shown in Fig. 1. Notice that the freezing temperature shifts by about 5 K in the range of frequencies

^{a)} Electronic mail: flam@df.ufpe.br

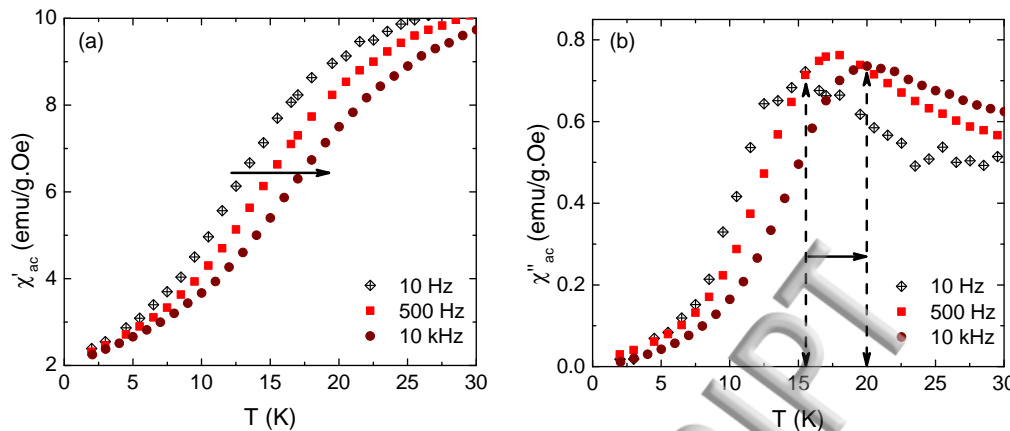


FIG. 1. (color online) Temperature dependence of the χ'_{ac} (in-phase) (a) and χ''_{ac} (out-of-phase) (b) components of the magnetic susceptibility of $\text{Fe}_{90}\text{Zr}_{10}$ for $f = 10, 500$ and 10^4 Hz and for $h_{ac} = 5$ Oe. The data for χ''_{ac} reveals that the freezing temperature shifts by about 5 K when f varies in the range $10 - 10^4$ Hz. The arrows indicate the direction of increasing f .

covered by the experiments as previously reported.¹⁷

For the magnetoimpedance (Z) measurements we have used the same melt spun ribbon of $\text{Fe}_{90}\text{Zr}_{10}$ with dimensions 8.9 mm long, 0.7 mm wide and $9.0 \mu\text{m}$ thick.¹⁰⁰ The electric contacts were made with silver paint. The impedance was measured using a standard four terminal measurement technique. The schematics of the experimental set-up and typical magnetoimpedance data are shown in Fig. 2. The data acquisition is fully automated with LabView software (National Instruments) controlling a high frequency lock-in amplifier (Stanford Research model SR844) via a GPIB interface. The magnitude of the ac electrical current was maintained at 13 mA while the frequencies of the electric current were 5, 10 and 15¹⁰⁵ MHz. A closed cycle refrigerator (Displex) was used to vary the temperature between 10 and 300 K. An applied magnetic field, H , was swept in the range ± 6.0 kOe at each measurement temperature. The magnetoimpedance data were corrected for the transmission lines connecting the lock-in amplifier to the sample at the cold tip (coaxial cables outside and twisted pairs inside the Displex). The magnetoimpedance data shown in Fig. 2 have a maximum Z near $H = 0$ and effectively saturates at ± 6.0 kOe. The upper left inset is a blow-up of the central part of the Z vs H curve while the right inset is a block diagram of the experimental set-up.

Figure 3 shows a 3D plot of the variation of $\Delta Z(H, T) = Z(H, T) - Z(H_{max}, T)$ as a function of H and T . The important features in this figure include the fact the magnetoimpedance is largest at zero applied field, is essentially saturated and constant at H_{max} , begins a rapid increase at T_C , about 225 K, reaches a maximum at around 160 K and decreases more slowly for lower temperatures.

A plot of the maximum GMI percentage occurring at $H = 0$ is shown as a function of T in Fig. 4 along with, for comparison, the dc electric resistivity. $\rho(T)$ varies by

less than 4% and increases monotonically with decreasing T below T_C . The T -dependence of the electrical resistivity and of the magneto-resistance for samples with similar concentration have also been investigated in the past.¹⁸⁻²⁰ It was found that the magneto-resistance varies by less than 0.5% even for higher values of applied magnetic fields (up to 8 T). Thus, the magneto-resistance is not relevant in determining the GMI in this sample material. Moreover, the minimum in the electrical resistance near T_C was found to be due to coherent exchange scatterings rather than to the more usual Kondo effect.²⁰ As is evident in this figure, the temperature dependence of the GMI has some interesting features not seen in $\rho(T)$. First, it has a maximum value of about 15%

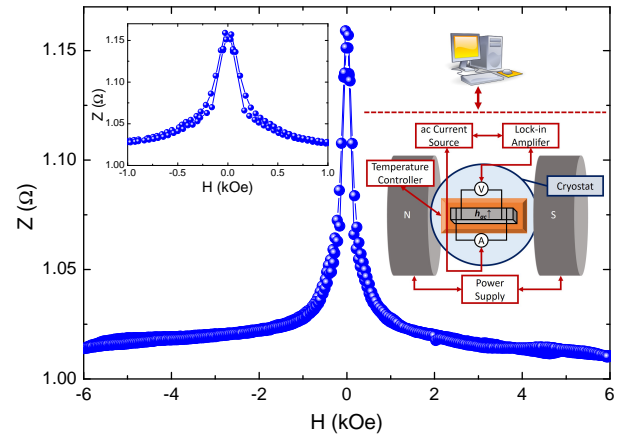


FIG. 2. (color online) Typical Z vs H data for $I_{ac} = 13$ mA, $f = 15$ MHz and $T = 150$ K. The upper left inset is a blow-up of the central part of the curve while the right inset shows a block diagram of the experimental set-up used in the GMI measurements.

close to 160 K. This maximum is strongly correlated with the one observed in the magnetic permeability which, in turn, follows the trends observed in both dc and ac magnetic susceptibility data.¹⁷ Moreover, the GMI decreases monotonically with T and there is a change in the slope in the low- T regime. It is also interesting to notice that the competing ferro-antiferromagnetic interactions evidenced in the dc and ac magnetic susceptibility does also makes the GMI to diminish with T even before the spin-glass phase is reached. This effect is more pronounced below about 50 K and it is also present in $\rho(T)$.

The temperature dependence of the penetration-depth δ was determined for each frequency using the theoretical model of the impedance for soft-ferromagnetic ribbons⁹

$$\left| \frac{(1-i)l}{2w\delta} \frac{\rho}{1-e^{-(1-i)d/2\delta}} \right| - Z = 0 \quad (1)$$

where l , w and d are, respectively, the length, width and thickness of the ribbon. The temperature dependence of the transverse ac magnetic permeability $\mu_T = \rho/\pi f \delta^2$ is then obtained from δ . (Note it is the transverse permeability measured since the high frequency magnetic field is orthogonal to the swept field.)

Figure 5 shows the data for both $\delta(T)$ and μ_T for 15 MHz. The $\mu_T(T)$ data is normalized by the permeability of vacuum ($\mu_0 = 4\pi \times 10^{-7} \text{ H/m}$) and its T -dependence follows closely the trends observed in the GMI data. Well above T_C it is small, as expected, and increases as the temperature is reduced below T_C . It exhibits a maximum at about 160 K and then decreases monotonically with decreasing temperature.

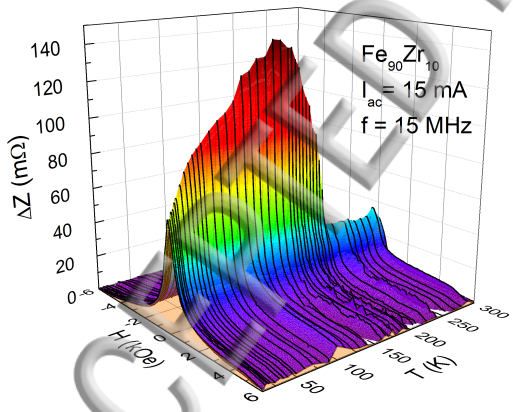


FIG. 3. (color online) $\Delta Z(H, T) = (Z(H) - Z(H_{max}))$ as a function of H and T . Notice that ΔZ diminishes rapidly above T_C and monotonically for low values of T .

In order to investigate the behavior of the freezing temperature in the MHz frequency range, the ac magnetic susceptibility $\chi_{ac} = \mu_T - 1$ was calculated for 5, 10 and 15 MHz in the temperature range 10 - 50 K. The cross over temperature from the ferromagnetic to the spin-glass

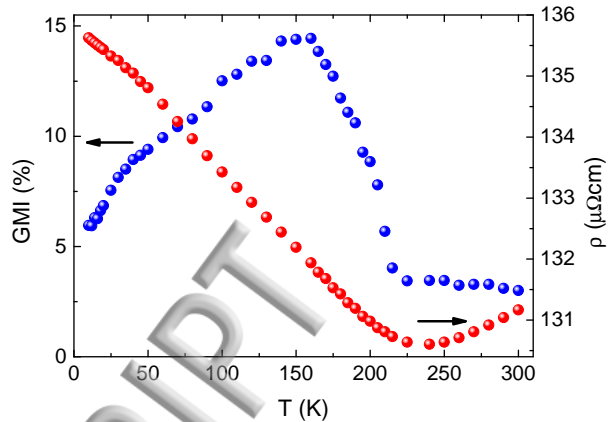


FIG. 4. (color online) GMI and ρ versus temperature data for $f = 15$ MHz. The maximum GMI is about 15% while ρ varies less than 4% in the full range of T .

phase is better seen if one plots the log of χ_{ac} vs. T as shown in the inset of Fig. 6 for $f = 5$ MHz. The intercept of linear fits to the data above and below the crossing temperature yields the glassy temperature T_f for a given f ($= T_g(f)$). For the three frequencies, 5, 10 and 15 MHz, we find values of T_f of 27.8, 28.4 and 30.1 K, respectively.

Shown in Fig. 6 is a log-log plot of the relaxation time τ ($= 1/f$) versus reduced temperature $t_r = T_f/T_g - 1$ with $T_g = 14.0$ K. Notice that the plot includes the values of τ obtained from the GMI data ($f = 5, 10$ and 15 MHz) and the set obtained from the χ_{ac} data measured below 10 kHz. It is interesting to notice that the spin-dynamics follows a typical power-law behavior even for values of τ close to 10^{-8} s. This is the first report of such short values since previous efforts have been limited to values

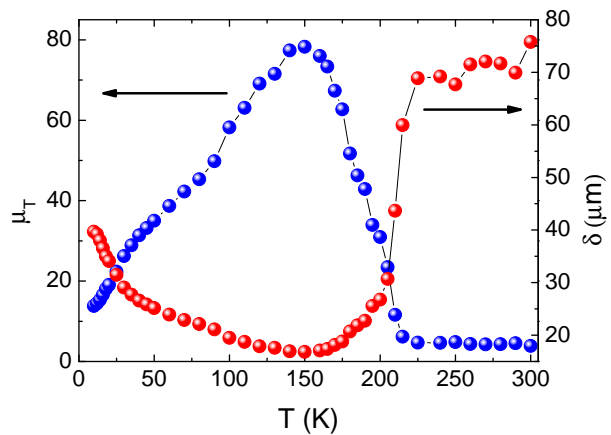


FIG. 5. (color online) Transverse ac magnetic permeability μ_T and penetration-depth δ versus temperature for $f = 15$ MHz.

¹⁶ determined from χ_{ac} data. The blue dashed and solid lines in Fig. 6 represent fittings to the power-law function¹⁹⁵ $\tau = \tau_0 z^{\nu}$ typical of standard critical slowing down²¹ in spin glass systems, where ν and z are, respectively, the correlation length and the dynamical critical exponent, and τ_0 is a microscopic relaxation time. The data show a crossover between two regimes, labeled 1, with $3.3 \times 10^{-3} \leq \tau \leq 1.0 \times 10^{-1}$ s and a high temperature regime, labeled 2, with $6.7 \times 10^{-8} \leq \tau \leq 3.3 \times 10^{-3}$ s. A best fit of the power law to the data in regime 1 was obtained using $z\nu = 2.6$ and $\tau_0 = 1.1 \times 10^{-4}$ s. Those values are far from usual values for spin-glass systems. This is²⁰⁵ compared to those for regime 2 where the best fit yields $z\nu = 7.4$ and $\tau_0 = 1.6 \times 10^{-7}$ s, which are very close to the ones obtained for other spin-glass like systems.²²

²¹⁵ Moreover $z\nu$ in regime 2 is in good agreement with the values predicted by Monte Carlo simulations²³ and by²¹⁰ renormalization group calculations²⁴ for short range Ising spin glasses. Notice also that the shift in T_f per decade of frequency, given by $\Delta T_f/T_g \Delta \log(f)$, for regime 2 was found to be about 0.17. This is a somewhat large value and it is about 5 times the value obtained by using low frequency data only.²⁵ An attempt was made to fit a²¹⁵ Voguel-Fulcher law²⁶ but a good fit for the full range of relaxation times was not found. Finally we note that the existence of more than one regime in the spin dynamics in reentrant spin-glass phases has also been observed in²²⁰ other ferromagnetic alloys.²⁷

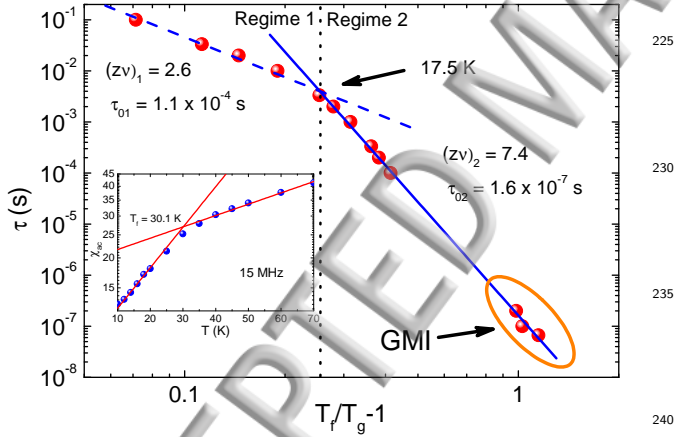


FIG. 6. (color online) τ vs. reduced freezing temperature. For $\tau \geq 10^{-4}$ s the data were extracted from the χ_{ac} measured in the PPMS while the shortest ones are from the χ_{ac} obtained²⁴⁵ from the GMI data. The blue line is a fit to a power-law. The inset shows a log plot of χ_{ac} vs. T for $f = 5$ MHz. The solid red lines are linear fittings used for determining T_f .

depth associated to the magnetic field created by the ac electric current. The high- f χ_{ac} data were combined with the data measured for f in the range 10 - 10^4 Hz for testing the validity of the power-law description for the spin dynamics in spin-glass systems up to very short relaxation times. It was found that the dynamics follows two distinct regimes: one for long relaxations times ($\tau \leq 3.3 \times 10^{-3}$ s) and the other for short values ($6.7 \times 10^{-8} \leq \tau \leq 3.3 \times 10^{-3}$ s). For this latter regime, we find the critical exponent $z\nu = 7.4$ and the microscopic relaxation time $\tau_0 = 1.6 \times 10^{-7}$ s that are close to values obtained for other spin-glass-like systems.

Acknowledgments: This work was partially supported by the Brazilian Funding Agencies CNPq, CAPES, FACEPE and FINEP, the American Physical Society, and DOE Award Number: DE-SC0013599.

- ¹M. Gabay and G. Toulouse, *Phys. Rev. Lett.* **47**, 201 (1981).
- ²M. Wittmann and A. P. Young, *J. Stat. Mec.: Theory and Experiment* **2016**, 013301 (2016).
- ³I. A. Campbell, S. Senoussi, F. Varret, J. Teillet, and A. Hamzić, *Phys. Rev. Lett.* **50**, 1615 (1983).
- ⁴R. V. Chamberlin, *Phys. Rev. Lett.* **83**, 5134 (1999).
- ⁵F. C. Montenegro, S. M. Rezende, and M. D. CoutinhoFilho, *J. Appl. Phys.* **63**, 3755 (1988); F. C. Montenegro, U. A. Leitão, M. D. Coutinho-Filho, and S. M. Rezende, *J. Appl. Phys.* **67**, 5243 (1990).
- ⁶K. Binder and A. P. Young, *Rev. Mod. Phys.* **58**, 801 (1986).
- ⁷F. L. A. Machado, B. L. da Silva, S. M. Rezende, and C. S. Martins, *J. Appl. Phys.* **75**, 6563 (1994).
- ⁸F. L. A. Machado, C. S. Martins, and S. M. Rezende, *Phys. Rev. B* **51**, 3926 (1995).
- ⁹F. L. A. Machado and S. M. Rezende, *J. Appl. Phys.* **79**, 6558 (1996).
- ¹⁰M. H. Phan and H. X. Peng, *Prog. Mater. Science* **53**, 323 (2008).
- ¹¹M. Kurniawan, R. K. Roy, A. K. Panda, D. W. Greve, P. Ohodnicki, and M. E. McHenry, *J. of Elect. Mater.* **43**, 4576 (2014).
- ¹²D. Karnaushenko, D. D. Karnaushenko, D. Makarov, S. Baunack, R. Schfer, and O. G. Schmidt, *Adv. Materials* **27**, 6582 (2015).
- ¹³H. Hiroyoshi and K. Fukamichi, *Phys Lett. A* **85**, 242 (1981).
- ¹⁴H. Hiroyoshi and K. Fukamichi, *J. Appl. Phys.* **53**, 2226 (1982).
- ¹⁵D. Kaptys, T. Kemny, L. Kiss, L. Grnsy, J. Balogh, and I. Vincze, *J. Non-Cryst. Solids* **156**, 336 (1993).
- ¹⁶D. H. Ryan, J. M. D. Coey, E. Batalla, Z. Altounian, and J. O. Ström-Olsen, *Phys. Rev. B* **35**, 8630 (1987).
- ¹⁷P. R. T. Ribeiro, F. L. A. Machado, and E. Dan Dahlberg, *J. Appl. Phys.* **117**, 17E124 (2015).
- ¹⁸Y. Obi, L. C. Wang, R. Motsay, D. G. Onn, and M. Nose, *J. Appl. Phys.* **53**, 2304 (1982).
- ¹⁹K. Fukamichi, R. J. Gambino, and T. R. McGuire, *J. Appl. Phys.* **53**, 2310 (1982).
- ²⁰D. Dahlberg, K. V. Rao, and K. Fukamichi, *J. Appl. Phys.* **55**, 1942 (1984).
- ²¹P. C. Hohenberg and B. I. Halperin, *Rev. Mod. Phys.* **49**, 435 (1977).
- ²²R. B. da Silva, J. H. de Araújo, J. M. Soares, and F. L. A. Machado, *J. Appl. Phys.* **115**, 113906 (2014).
- ²³A. T. Ogielski, *Phys. Rev. B* **32**, 7384 (1985).
- ²⁴R. Riera and J. A. Hertz, *J. Phys. A: Math. and Gen.* **24**, 2625 (1991).
- ²⁵J. Nogus and K. Rao, *J. Mag. Mag. Mater.* **135**, L11 (1994).
- ²⁶J. Tholence, *Solid Sta/ Commun.* **35**, 113 (1980).
- ²⁷B. H. Verbeek, G. J. Nieuwenhuys, H. Stocker, and J. A. Mydosh, *Phys. Rev. Lett.* **40**, 586 (1978).

